Carbon Electrodes

DOI: 10.1002/ange.201300312

Bioinspired Wafer-Scale Production of Highly Stretchable Carbon Films for Transparent Conductive Electrodes**

Rongjin Li, Khaled Parvez, Felix Hinkel, Xinliang Feng, and Klaus Müllen**

Flexible transparent and conductive films (TCFs) are essential elements of the next-generation flexible devices, including touch screens and displays, organic light-emitting diodes (OLEDs), solar cells (SCs), organic field-effect transistors (OFETs), and sensors.[1] Indium tin oxide (ITO) has been the most widely used TCF in optoelectronic devices for almost four decades, owing to its low sheet resistance ($R_s \approx 10\ \Omega/\square$) coupled with high transmittance ($T \approx 80\,\%$). However, ITO suffers from inherent brittleness, which makes it unsuitable for flexible devices. In the race to replace ITO, networks of metal nanowires[2] and carbon nanotubes[3] are leading the pack; however, their high costs of synthesis and high surface roughness hamper their commercial applications.[1a,4] Graphene and graphene-based thin films have been recognized as attractive alternatives because of their outstanding electronic, optoelectronic, and mechanical properties.[5] Although sheet resistance as low as 30 $\Omega/\square$ (at $T = 90\,\%$) has been obtained for graphene grown on metallic substrates,[6] the multi-transfer process associated with the additional chemical doping increases the costs dramatically. The establishment of facile, yet controllable methods for the large-area production of flexible TCFs at low costs remains a challenging task.

The molecular precursor approach,[7] namely the production of carbon-based TCFs using aromatic-rich precursors as the carbon source seems to be much less explored. Through the thermal treatment of properly selected organic precursors, this synthetic method offers an intriguing means to low-costs processing and structural control of highly conductive carbon/graphene films,[7,8] which are difficult to achieve using methods such as chemical vapor deposition (CVD),[6,9] epitaxial growth,[10] liquid exfoliation,[11] and reduction of graphene oxide (GO) film.[12] Nevertheless, the bottleneck associated with this method lies in the relatively low electrical conductivity of the produced TCFs (e.g., 206 $S\,cm^{-1}$ for a pyrolyzed film of a giant polycyclic aromatic hydrocarbon[7]).

Recently, inspired by the adhesive proteins secreted by marine mussels, polydopamine (PDA) has proven to be a material for facile and universal surface coating.[13] By self-polymerization of dopamine, PDA that sticks to the surface of virtually all types of solid materials regardless of their chemical nature, can be produced.[13,14] The self-polymerization reaction is so mild that simple immersion of substrates in an aqueous solution of dopamine results in the spontaneous deposition of PDA film.[13,14] The film is layer-structured[15] and the thickness can be tailored at the nanometer scale.[13] PDA is mainly composed of cross-linked indolequinone units[16] (Figure 1, the definitive atomic scale structure of PDA remains elusive), thus making it a promising carbon and nitrogen-rich precursor for the construction of TCFs. Herein, we report the wafer-scale production of highly stretchable TCFs employing dopamine as the precursor (Figure 1). Pyrolyzed PDA films (PPD film) can be directly fabricated on dielectric surfaces or transferred to plastic substrates. PPD films are highly conductive and transparent, and can reversibly withstand mechanical deformations (such as being stretched to 20 % for 100 cycles). Solution-processed OFETs applying patterned PPD electrodes demonstrate significant increases in charge–carrier mobility compared with conventional gold-based electrodes. The remarkable application of PPD films as transparent flexible electrodes is further demonstrated by the fabrication of bendable polymer photodetectors, which exhibit no performance degradation when the devices are bent to a radius of about 1.5 mm for 100 cycles.

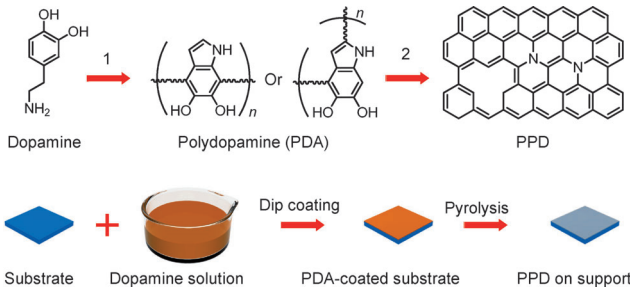

Figure 1. Chemical structures of dopamine, PDA, and PPD (model), and the procedures for the synthesis of PPD film. 1) Self-polymerization. 2) Pyrolysis at elevated temperature.

By simple immersion of the target substrates (e.g., SiO_2/Si or Cu foil in this study) in an aqueous solution of dopamine (2 mg of dopamine per milliliter of 10 mM tris-(hydroxy-

[*] Dr. R. Li, K. Parvez, F. Hinkel, Prof. Dr. X. Feng, Prof. Dr. K. Müllen
Max Planck Institute for Polymer Research
Ackermannweg 10, Mainz, 55128 (Germany)
E-mail: feng@mpip-mainz.mpg.de
muellen@mpip-mainz.mpg.de
Prof. Dr. X. Feng
School of Chemistry and Chemical Engineering
Shanghai Jiao Tong University
Shanghai, 200240 (P.R. China)

[**] Financial support by the ERC grant on NANOGRAPH, ENERCHEM, DFG Priority Program SPP 1459, BMBF LiBZ, ESF Project GOSPEL (Ref Nr: 9-EuroGRAPHENE-FP-001), EU Project GENIUS, and MOLESOL. The authors thank Haixin Zhou for the TEM measurements, Dr. Zhong-shuai Wu for the SEM measurements, and Dr. Xianjie Liu (Linköping University) for the XPS measurements.

Supporting information for this article is available on the WWW under http://dx.doi.org/10.1002/anie.201300312.

methyl) aminomethan, pH 8.5), PDA films were readily deposited on the surfaces.[13] The thickness of the film could be controlled by the immersion time (see Figure S1 in the Supporting Information). PDA-coated substrates were then placed in a tube furnace for thermal treatment at elevated temperatures in a hydrogen atmosphere (see the Supporting Information).

Atomic force microscopy (AFM) images of PPD films revealed a low surface roughness (R_a) of 0.60 nm over an area of $2\times2\ \mu m^2$ on SiO_2/Si substrate (Figure 2a). As expected the

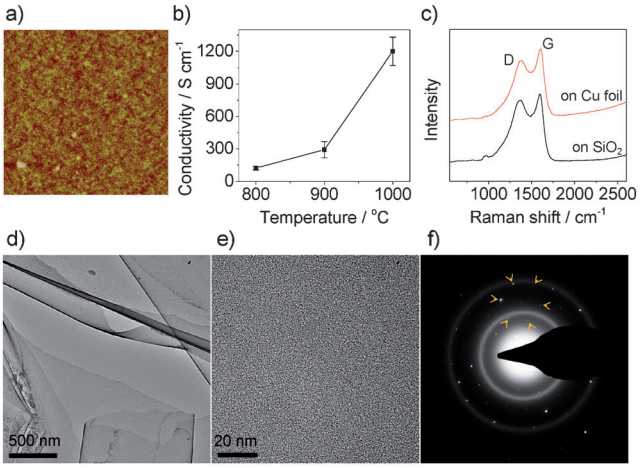

Figure 2. a) Tapping-mode AFM image of a PPD film on SiO_2/Si substrate. The area is $2\times2\ \mu m^2$ and the thickness of the film is about 10 nm. b) Conductivity as a function of pyrolysis temperature from 800 to 1000 °C. c) Raman spectra of a PPD film on SiO_2 and Cu foils. d–e) TEM images of a PPD film. f) SAED pattern of a PPD film. One hexagonal diffraction pattern is indicated.

electrical conductivity of PPD films is highly dependent on the pyrolysis temperature (Figure 2b). Remarkably, treatment at 1000 °C gave an average conductivity as high as 1200 S cm^{-1}. This value is comparable to that of polycrystalline graphite (1250 S cm^{-1})[17] and much higher than that of reduced graphene oxide (RGO) (e.g. 727 S cm^{-1}, 1100 °C)[12f] and pyrolyzed polycyclic aromatic hydrocarbon (206 S cm^{-1}, 1100 °C).[7] Furthermore, we found that the conductivity of PPD films was independent of the film thickness within the range of 3.4–20.5 nm (Figure S3 in the Supporting Information).

PPD films showed identical Raman spectra on SiO_2 and Cu foils (at 488 nm, 2 mW incident power, Figure 2c). The two peaks, one at approximately 1590 cm^{-1} and the other at 1360 cm^{-1}, were assigned to the G (graphitic carbon) and D bands (disordered carbon), respectively. The pronounced G peak, in comparison to the D peak ($I_D/I_G = 0.9$), indicated the good graphitic nature of the PPD film, which is likely responsible for the high conductivity.[18] Nevertheless, the presence of the D peak suggested that a certain number of defects were present in the PPD film which may be due to the doping by heteroatoms (nitrogen and oxygen) and the incorporation of pentagons and heptagons in the graphitic planes during the graphitization of PDA.

The morphology and microstructure of the PPD films were further characterized by transmission electron microscopy (TEM). Remarkably enough, the films were continuous (Figure 2d) without any noticeable pinholes or cracks at the hundred-nanometer scale (Figure 2e). The typical selected area electron diffraction (SAED) pattern revealed both diffraction rings and ordered hexagonal diffraction patterns (Figure 2f). In some regions, only ordered hexagonal diffraction patterns were observed (see Figure S4 in the Supporting Information). On the basis of these results, PPD may be regarded as a multi-layered graphene-constructed film. This coincides with the graphitic nature of the film deduced from the Raman and X-ray photoelectron spectra (Figures S5–7 and Tables S1–3 in the Supporting Information for the XPS analysis). The smooth and continuous morphology, together with the graphitic nature further, supported the high conductivity of the PPD film.

Owing to the versatile coating ability of PDA films, they can be readily produced on sacrificial metal foils and are transferrable to arbitrary substrates. In this study, PDA films of different thicknesses (from about 2.0 to 20.0 nm) were fabricated on Cu foil, thermally treated at 1000 °C (Figure 3a)

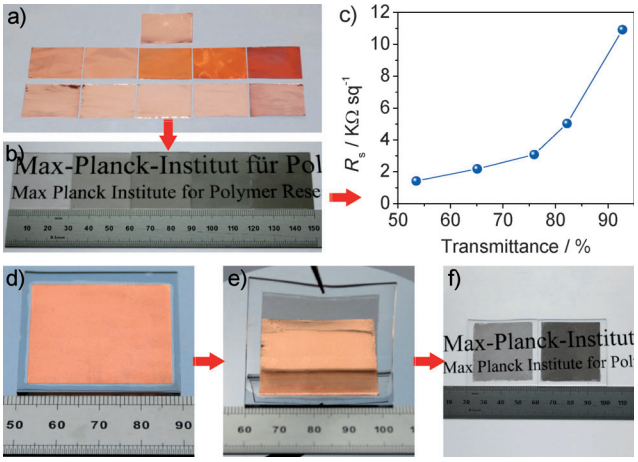

Figure 3. a) Dip-coating of a PDA film on a Cu foil. The top sheet is a pristine Cu foil. The five pieces in the middle are Cu foils dip-coated for 2.5, 6, 12, 24, and 48 h, respectively, and the bottom five pieces are the corresponding pyrolyzed ones. b) PPD film transferred on PET substrate with transmittance from 53.5 to 92.8% (at 550 nm). The films are 3×3 cm^2. c) Sheet resistance–transmittance curve of the samples on PET. d–e) Procedures of the "direct dry-transfer" method. f) PPD films of different transmittances transferred to PDMS sheets by the "direct dry-transfer" method.

and transferred onto a polyethylene terephthalate (PET) substrate employing polymethylmethacrylate (PMMA) as the supporting layer (Figure 3b).[9c,19] Only a single transfer was required to obtain films of different thicknesses (Figure 3b, corresponding transmittance from 92.8 to 53.5%), representing a great advantage over CVD-graphene, where repeated transfer processes are required to produce a few-layer film.[6,9a] The relationship between R_s and T is displayed in Figure 3c. A sheet resistance of 5.0 KΩ/□ was obtained at a transmittance of 82.0%, which was much lower than the

pyrolyzed PAH films on quartz ($R_s = 18\ K\Omega/\square$ at $T = 85.0\%$). In addition to the facile thickness control, large-area production is also possible. For example, a wafer-scale film was easily fabricated on plastic substrates (e.g., $7 \times 7\ cm^2$ film on PET, Figure S8 in the Supporting Information) and the size of the film was only limited by the diameter of the tube furnace used in our experiment.

We further developed a "direct dry-transfer" method for the clean and fast transfer of PPD film to plastic substrates. Owing to the low surface energy of polydimethylsiloxane (PDMS),[20] slight pressure applied to one edge of the PDMS substrate initiated contact with the PPD film on a Cu foil; van der Waals forces then spontaneously induced a "wetting" front which proceeded across the interface until fully contacted (Figure 3d). After peeling off the PDMS sheet (Figure 3e), successful transfer of a PPD film from the Cu foil to PDMS was achieved. Applying this method, PPD films of different transmittances (e.g., $T = 81.2$ and 50.5% in Figure 3f) were deposited on the PDMS substrate. This transfer method is contamination-free, as no supporting film or etchant solution was involved, and the entire transfer process was carried out within several minutes.

To investigate the stretchability of PPD films, the "direct dry-transfer" method was employed to prepare the samples on PDMS substrate ($T = 62.6\%$). The resistance increased almost linearly when the film was stretched from 0 to 20% (Figure 4a). Remarkably, the resistance perfectly resumed to

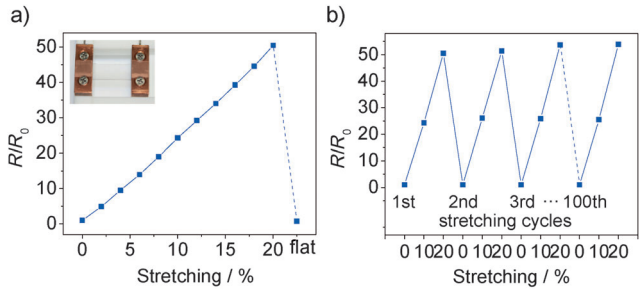

Figure 4. a) Variation in resistance of a PPD film stretched to 20% ($T = 62.6\%$). The inset shows the photograph during the stretching test. b) Variation in resistance of a PPD film stretched to 20% for 100 cycles.

the original value (R_0, on flat unstretched PDMS) after recovering the film to the flat state. Furthermore, the stretching to 20% was tested for 100 cycles without any noticeable change in resistance in the unstretched state (Figure 4b and Supporting Information Video S1). When the PPD/PDMS film was stretched to 30%, it was unable to recover to its original state, possibly due to the mechanical cracking of the PDMS. In contrast, CVD-graphene transferred to an unstrained PDMS substrate only demonstrated stretchability up to about 6%.[9b] Therefore, in our study, PPD films exhibited pronounced stretching stability with respect to CVD-graphene, indicating their potential application as flexible TCFs.

Encouraged by the outstanding electrical conductivity, PPD films on SiO_2/Si were examined as electrodes for OFETs. A PPD film was first patterned as source–drain electrodes as described previously.[21] A semiconducting polymer CDT-BTZ-C16 ($M_w = 10$ KDa, polydispersity index = 2.67)[22] was then drop-cast on the patterned electrodes. Remarkably, a hole mobility as high as $0.8\ cm^2 V^{-1} s^{-1}$ was obtained, which is eight times higher than that using gold-based source–drain electrodes (Figure S9 in the Supporting Information). Furthermore, taking advantage of the high stretchability of the PPD films, we fabricated flexible photodetectors using PPD as transparent electrodes. PPD patterns (channel length 50 μm, width 20 mm, Figure S10 in the Supporting Information) were transferred from a Cu foil to PET or PDMS (Figure 5a,b). A blend of poly(3-hexylthio-

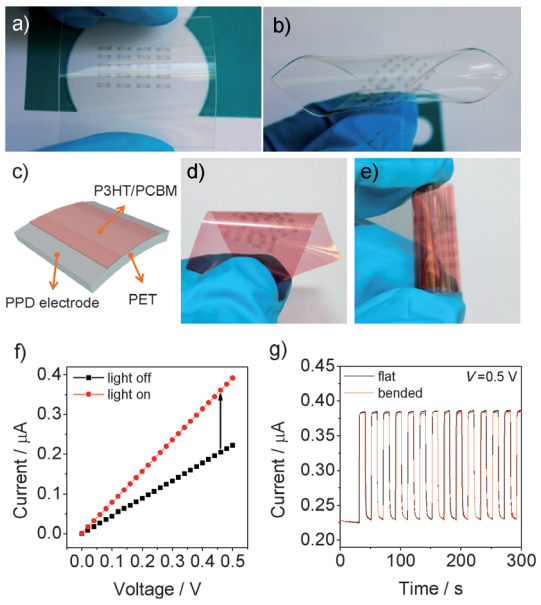

Figure 5. a) Patterned PPD film on PET and b) PDMS. c) Flexible photodetector on PET substrate with PPD as the electrode. d–e) Photograph of the photodetector when it was bent and curled. The device was semi-transparent after the coating of the P3HT:PCBM layer. f) *I–V* characteristics of the photodetector. g) The on/off characteristics of the photodetector in the flat and bent state.

phene) (P3HT) with phenyl-C61-butyric acid methylester (PCBM)[23] was spin-coated on a PET substrate bearing the patterned PPD electrodes (Figure 5c). The device was bendable and could even be rolled up (Figure 5d,e). In the current–voltage (*I–V*) curves (Figure 5f) the current increased markedly upon light irradiation (about $20\ mW\,cm^{-2}$). When a bias voltage was applied (e.g., 0.5 V in this study), the device exhibited fast and repeatable responses to light (Figure 5g). Remarkably, after bending the device to a radius of about 1.5 mm (tensile strain of 0.8%) for 100 cycles, the photodetector showed no obvious change in light response in the bent state compared with its original performance, indicating again the great potential of PPD as a flexible electrode.

In conclusion, we have developed a bioinspired approach to the wafer-scale production of highly stretchable precursor-constructed TCFs using dopamine as the carbon source. The

versatile coating ability of PDA enables the production of PPD films on both dielectric substrates for devices and the transfer of the film to plastic substrates for flexible devices. The use of solid precursors provides a facile yet controllable way to produce TCFs, which will allow profitable, large-scale industrial manufacturing.

Received: January 14, 2013
Published online: April 16, 2013

Keywords: carbon · carbon electrodes · dopamine · graphene · molecular devices

[1] a) D. S. Hecht, L. Hu, G. Irvin, *Adv. Mater.* **2011**, *23*, 1482 – 1513; b) A. Kumar, C. Zhou, *ACS Nano* **2010**, *4*, 11 – 14.

[2] a) H. Wu, L. Hu, M. W. Rowell, D. Kong, J. J. Cha, J. R. McDonough, J. Zhu, Y. Yang, M. D. McGehee, Y. Cui, *Nano Lett.* **2010**, *10*, 4242 – 4248; b) S. De, T. M. Higgins, P. E. Lyons, E. M. Doherty, P. N. Nirmalraj, W. J. Blau, J. J. Boland, J. N. Coleman, *ACS Nano* **2009**, *3*, 1767 – 1774; c) J.-Y. Lee, S. T. Connor, Y. Cui, P. Peumans, *Nano Lett.* **2008**, *8*, 689 – 692; d) M.-G. Kang, M.-S. Kim, J. Kim, L. J. Guo, *Adv. Mater.* **2008**, *20*, 4408 – 4413.

[3] a) S. H. David, M. H. Amy, L. Roland, H. Liangbing, M. Bryon, C. Chad, R. Steven, *Nanotechnology* **2011**, *22*, 075201; b) E. M. Doherty, S. De, P. E. Lyons, A. Shmeliov, P. N. Nirmalraj, V. Scardaci, J. Joimel, W. J. Blau, J. J. Boland, J. N. Coleman, *Carbon* **2009**, *47*, 2466 – 2473; c) H.-Z. Geng, K. K. Kim, K. P. So, Y. S. Lee, Y. Chang, Y. H. Lee, *J. Am. Chem. Soc.* **2007**, *129*, 7758 – 7759; d) Z. Wu, Z. Chen, X. Du, J. M. Logan, J. Sippel, M. Nikolou, K. Kamaras, J. R. Reynolds, D. B. Tanner, A. F. Hebard, A. G. Rinzler, *Science* **2004**, *305*, 1273 – 1276; e) L. Hu, D. S. Hecht, G. Grüner, *Nano Lett.* **2004**, *4*, 2513 – 2517.

[4] S. De, J. N. Coleman, *ACS Nano* **2010**, *4*, 2713 – 2720.

[5] a) M. Liang, J. Wang, B. Luo, T. Qiu, L. Zhi, *Small* **2012**, *8*, 1180 – 1184; b) J. Wang, M. Liang, Y. Fang, T. Qiu, J. Zhang, L. Zhi, *Adv. Mater.* **2012**, *24*, 2874 – 2878; c) S. Pang, Y. Hernandez, X. Feng, K. Müllen, *Adv. Mater.* **2011**, *23*, 2779 – 2795; d) F. Bonaccorso, Z. Sun, T. Hasan, A. C. Ferrari, *Nat. Photonics* **2010**, *4*, 611 – 622; e) A. K. Geim, *Science* **2009**, *324*, 1530 – 1534; f) R. R. Nair, P. Blake, A. N. Grigorenko, K. S. Novoselov, T. J. Booth, T. Stauber, N. M. R. Peres, A. K. Geim, *Science* **2008**, *320*, 1308; g) C. Lee, X. Wei, J. W. Kysar, J. Hone, *Science* **2008**, *321*, 385 – 388; h) A. K. Geim, K. S. Novoselov, *Nat. Mater.* **2007**, *6*, 183 – 191; i) K. S. Novoselov, A. K. Geim, S. V. Morozov, D. Jiang, M. I. Katsnelson, I. V. Grigorieva, S. V. Dubonos, A. A. Firsov, *Nature* **2005**, *438*, 197 – 200; j) K. S. Novoselov, A. K. Geim, S. V. Morozov, D. Jiang, Y. Zhang, S. V. Dubonos, I. V. Grigorieva, A. A. Firsov, *Science* **2004**, *306*, 666 – 669.

[6] S. Bae, H. Kim, Y. Lee, X. Xu, J.-S. Park, Y. Zheng, J. Balakrishnan, T. Lei, H. Ri Kim, Y. I. Song, Y.-J. Kim, K. S. Kim, B. Ozyilmaz, J.-H. Ahn, B. H. Hong, S. Iijima, *Nat. Nanotechnol.* **2010**, *5*, 574 – 578.

[7] X. Wang, L. Zhi, N. Tsao, Ž. Tomović, J. Li, K. Müllen, *Angew. Chem.* **2008**, *120*, 3032 – 3034; *Angew. Chem. Int. Ed.* **2008**, *47*, 2990 – 2992.

[8] a) F. Guo, A. Mukhopadhyay, B. W. Sheldon, R. H. Hurt, *Adv. Mater.* **2011**, *23*, 508 – 513; b) P. R. Somani, S. P. Somani, M. Umeno, *Chem. Phys. Lett.* **2006**, *430*, 56 – 59; c) L. Zhi, J. Wu, J. Li, U. Kolb, K. Müllen, *Angew. Chem.* **2005**, *117*, 2158 – 2161; *Angew. Chem. Int. Ed.* **2005**, *44*, 2120 – 2123.

[9] a) X. Li, Y. Zhu, W. Cai, M. Borysiak, B. Han, D. Chen, R. D. Piner, L. Colombo, R. S. Ruoff, *Nano Lett.* **2009**, *9*, 4359 – 4363; b) K. S. Kim, Y. Zhao, H. Jang, S. Y. Lee, J. M. Kim, J. H. Ahn, P. Kim, J. Y. Choi, B. H. Hong, *Nature* **2009**, *457*, 706 – 710; c) X. Li, W. Cai, J. An, S. Kim, J. Nah, D. Yang, R. Piner, A. Velamakanni, I. Jung, E. Tutuc, S. K. Banerjee, L. Colombo, R. S. Ruoff, *Science* **2009**, *324*, 1312 – 1314; d) W. Cai, Y. Zhu, X. Li, R. D. Piner, R. S. Ruoff, *Appl. Phys. Lett.* **2009**, *95*, 123115.

[10] a) P. W. Sutter, J.-I. Flege, E. A. Sutter, *Nat. Mater.* **2008**, *7*, 406 – 411; b) C. Berger, Z. Song, X. Li, X. Wu, N. Brown, C. Naud, D. Mayou, T. Li, J. Hass, A. N. Marchenkov, E. H. Conrad, P. N. First, W. A. de Heer, *Science* **2006**, *312*, 1191 – 1196; c) T. Ohta, A. Bostwick, T. Seyller, K. Horn, E. Rotenberg, *Science* **2006**, *313*, 951 – 954.

[11] Y. Hernandez, V. Nicolosi, M. Lotya, F. M. Blighe, Z. Sun, S. De, I. T. McGovern, B. Holland, M. Byrne, Y. K. Gun'Ko, J. J. Boland, P. Niraj, G. Duesberg, S. Krishnamurthy, R. Goodhue, J. Hutchison, V. Scardaci, A. C. Ferrari, J. N. Coleman, *Nat. Nanotechnol.* **2008**, *3*, 563 – 568.

[12] a) J. Wu, M. Agrawal, H. c. A. Becerril, Z. Bao, Z. Liu, Y. Chen, P. Peumans, *ACS Nano* **2009**, *4*, 43 – 48; b) Q. Su, S. Pang, V. Alijani, C. Li, X. Feng, K. Müllen, *Adv. Mater.* **2009**, *21*, 3191 – 3195; c) H. A. Becerril, J. Mao, Z. Liu, R. M. Stoltenberg, Z. Bao, Y. Chen, *ACS Nano* **2008**, *2*, 463 – 470; d) G. Eda, G. Fanchini, M. Chhowalla, *Nat. Nanotechnol.* **2008**, *3*, 270 – 274; e) D. A. Dikin, S. Stankovich, E. J. Zimney, R. D. Piner, G. H. B. Dommett, G. Evmenenko, S. T. Nguyen, R. S. Ruoff, *Nature* **2007**, *448*, 457 – 460; f) X. Wang, L. Zhi, K. Müllen, *Nano Lett.* **2007**, *7*, 323 – 327.

[13] H. Lee, S. M. Dellatore, W. M. Miller, P. B. Messersmith, *Science* **2007**, *318*, 426 – 430.

[14] H. Lee, J. Rho, P. B. Messersmith, *Adv. Mater.* **2009**, *21*, 431 – 434.

[15] J. Kong, W. A. Yee, L. Yang, Y. Wei, S. Phua, H. G. Ong, J. M. Ang, X. Li, X. Lu, *Chem. Commun.* **2012**, *48*, 10316 – 10318.

[16] a) L. Zhang, J. Shi, Z. Jiang, Y. Jiang, S. Qiao, J. Li, R. Wang, R. Meng, Y. Zhu, Y. Zheng, *Green Chem.* **2011**, *13*, 300 – 306; b) F. Yu, S. Chen, Y. Chen, H. Li, L. Yang, Y. Chen, Y. Yin, *J. Mol. Struct.* **2010**, *982*, 152 – 161; c) M. d'Ischia, A. Napolitano, A. Pezzella, P. Meredith, T. Sarna, *Angew. Chem.* **2009**, *121*, 3972 – 3979; *Angew. Chem. Int. Ed.* **2009**, *48*, 3914 – 3921; d) X.-B. Yin, D.-Y. Liu, *J. Chromatogr. A* **2008**, *1212*, 130 – 136.

[17] R. O. Grisdale, *J. Appl. Phys.* **1953**, *24*, 1288 – 1296.

[18] a) A. C. Ferrari, J. C. Meyer, V. Scardaci, C. Casiraghi, M. Lazzeri, F. Mauri, S. Piscanec, D. Jiang, K. S. Novoselov, S. Roth, A. K. Geim, *Phys. Rev. Lett.* **2006**, *97*, 187401 – 187404; b) F. Tuinstra, J. L. Koenig, *J. Chem. Phys.* **1970**, *53*, 1126 – 1130.

[19] a) A. Reina, H. Son, L. Jiao, B. Fan, M. S. Dresselhaus, Z. Liu, J. Kong, *J. Phys. Chem. C* **2008**, *112*, 17741 – 17744; b) A. Reina, X. Jia, J. Ho, D. Nezich, H. Son, V. Bulovic, M. S. Dresselhaus, J. Kong, *Nano Lett.* **2008**, *8*, 30 – 35.

[20] a) V. C. Sundar, J. Zaumseil, V. Podzorov, E. Menard, R. L. Willett, T. Someya, M. E. Gershenson, J. A. Rogers, *Science* **2004**, *303*, 1644 – 1646; b) S. Perutz, J. Wang, E. J. Kramer, C. K. Ober, K. Ellis, *Macromolecules* **1998**, *31*, 4272 – 4276.

[21] S. Pang, H. N. Tsao, X. Feng, K. Müllen, *Adv. Mater.* **2009**, *21*, 3488 – 3491.

[22] M. Zhang, H. N. Tsao, W. Pisula, C. Yang, A. K. Mishra, K. Müllen, *J. Am. Chem. Soc.* **2007**, *129*, 3472 – 3473.

[23] a) H. Zhu, T. Li, Y. Zhang, H. Dong, J. Song, H. Zhao, Z. Wei, W. Xu, W. Hu, Z. Bo, *Adv. Mater.* **2010**, *22*, 1645 – 1648; b) S. Pang, S. Yang, X. Feng, K. Müllen, *Adv. Mater.* **2012**, *24*, 1566 – 1570.